UDC 539.215.9
IRSTI 29.19.31

https://doi.org/10.55452/1998-6688-2025-22-3-290-301

[1]Kadau A.T.,
Master's degree, ORCID ID: 0009-0008-9714-0304,
e-mail: aidoskadau@gmail.com
[1,2]Kalkozova Zh.K.,
Cand.Phys.-Math.Sc., Associate Professor, ORCID ID: 0000-0002-4826-1678,
e-mail: zhanar.kalkozova@kaznu.edu.kz
[1,3]*Gritsenko L.V.,
PhD, Associate Professor, ORCID ID: 0000-0003-0726-1118,
*e-mail: l.gritsenko@satbayev.university
[1,2]Markhabayeva A.A.,
PhD, ORCID ID: 0000-0002-0657-422X,
e-mail: aiko.marx87@gmail.com
[1,2]Abdullin Kh.A.,
Dr.Phys.-Math.Sc., Professor, ORCID ID: 0000-0002-2729-2272,
e-mail: kh.abdullin@physics.kz

[1]Institute of Applied Science & Information Technology, Almaty, Kazakhstan
[2]National nanotechnology laboratory of open type (NNLOT),
Al-Farabi Kazakh National university, Almaty, Kazakhstan
[3]Satbayev University, Almaty, Kazakhstan

INFLUENCE OF PARAMETERS OF LOW-COST SYNTHESIS METHODS ON ZINC OXIDE MORPHOLOGY

Abstract

The morphology of zinc oxide (ZnO) powders synthesised via a modified microwave assisted method under varying heating parameters, as well as by chemical bath deposition, was investigated. Image analysis revealed clear correlations between synthesis parameters and structural features. Increasing the microwave heating time at constant power led to a consistent transformation from loose nanoparticles to dense, well-faceted microstructures. In contrast, reducing heating power slowed crystallisation and agglomeration, preserving a finer, more porous structure. Scanning electron microscopy also demonstrated significant morphological differences in samples grown by chemical bath deposition, which were strongly influenced by the initial molar concentration of zinc acetate while keeping the concentrations of other solution components constant. These findings confirm that low-cost, environmentally friendly synthesis approaches can be used to control ZnO particle morphology through careful adjustment of precursor concentrations, heating time, and microwave power. Photocatalytic degradation tests of rhodamine B demonstrated a strong link between particle morphology and degradation rate. The highest rate (~0.5 h^{-1}) was recorded for a chemically precipitated sample, whereas the lowest (~0.1 h^{-1}) corresponded to a microwave-synthesised sample.

Keywords: zinc oxide, morphology, microwave assisted method, chemical bath deposition method, photocatalysis.

Introduction

Zinc oxide (ZnO) is a semiconductor material with a wide bandgap (~3.37 eV) that has attracted significant research interest owing to its unique optical, electronic, and catalytic properties [1–3]. Its high photostability, low toxicity, and relatively low cost make it suitable for a variety of applications, including solar cells, gas sensors, light-emitting diodes, and photocatalysis [4, 5]. One particularly

promising application is the degradation of organic dyes such as methylene blue, rhodamine B, and methyl orange and others, which are extensively used in the textile, paper, and food industries and pose serious environmental hazards when released into wastewater [6, 7].

The performance of a photocatalyst is largely determined by its morphology, particle size, and defect structure [8]. Recently, attention has shifted towards low-cost, energy-efficient methods for producing nanostructured ZnO, such as microwave synthesis and chemical bath deposition from aqueous solutions. These techniques allow precise control over morphology by varying parameters such as temperature, processing time, reagent concentrations, and pH [9, 10].

Microwave synthesis offers rapid, uniform heating, enabling the formation of finely dispersed, uniformly sized particles with high crystallinity [11]. It also minimises energy consumption and shortens processing time, making it a promising candidate for large-scale production [10, 11]. In comparison, the chemical bath deposition method is simple, cost-effective, and does not require sophisticated equipment [12, 13].

ZnO morphology directly influences photoinduced electron – hole pair generation and recombination [14, 15]. For example, nanorods and nanowires facilitate directional charge transport and reduce recombination rates, while porous and aggregated structures provide a high surface area for pollutant adsorption. Studies have shown that combining low-cost synthesis with surface modification can further enhance photocatalytic efficiency [16, 17].

Despite progress in the field, the influence of synthesis parameters, such as microwave irradiation power and duration, and solution composition and pH during precipitation on ZnO morphology and photocatalytic performance remains insufficiently explored. A systematic comparative study of these factors is needed.

This work presents a comparative analysis of ZnO samples synthesised by chemical bath deposition and microwave assisted methods under various conditions. It examines the effects of synthesis parameters on phase purity, texture, and crystallite size, and correlates these with photocatalytic activity in the degradation of rhodamine B.

Materials and methods

Two low-cost synthesis techniques were investigated: the chemical bath deposition method and a modified microwave assisted method. Both are attractive due to their accessibility, ease of implementation, and minimal equipment requirements. For the chemical bath deposition method, zinc acetate dihydrate ($Zn(CH_3\ COO)_2{\cdot}2H_2O$, Sigma-Aldrich), sodium hydroxide (NaOH, Sigma-Aldrich), and the anionic surfactant sodium dodecyl sulfate ($C_{12}H_{25}SO_4Na$) were used. Three sample compositions were studied: sample #CD1 (0.2 M $ZnAc_2$, 0.5 M NaOH and 10 mM surfactant), sample #CD2 (0.1 M $ZnAc_2$, 0.5 M NaOH and 10 mM surfactant), sample #CD3 (0.075 M $ZnAc_2$, 0.5 M NaOH and 10 mM surfactant). Zinc acetate was dissolved in 50 ml of distilled water and placed on a magnetic stirrer for homogenisation at 500 rpm without heating. Sodium hydroxide solution was prepared in the same way. NaOH was dissolved in 100 ml of distilled water and the solution was also stirred on a magnetic stirrer until complete homogenisation. During the stirring process, $(CH_3COO)_2Zn{\cdot}2H_2O$ and NaOH dissociate into ions according to formulae (1) and (2). Free hydroxide ions (OH^-) appear in the solution and participate in the precipitation of $Zn(OH)_2$. After both solutions became homogeneous they were mixed.

$$(CH_3COO)_2 \cdot 2H_2O \longrightarrow Zn^{2+} + 2CH_3COO^- + 2H_2O, \quad (1)$$

$$NaOH \longrightarrow Na^+ + OH^- \quad (2)$$

When solutions of zinc acetate and sodium hydroxide are mixed, zinc hydroxide precipitation reaction occurs according to formula (3)

$$Zn^{+} + OH^{-} \longrightarrow Zn(OH)_2 \downarrow. \quad (3)$$

$Zn(OH)_2$ is a white precipitate insoluble in water. The reaction occurs at a pH greater than 7, which is ensured by the presence of NaOH. When surfactant is added to the solution, it adsorbs on the surface of zinc hydroxide, preventing agglomeration of particles in solution [18]. The resulting solution was left on a magnetic stirrer at room temperature for a day to achieve complete homogeneity of the solution.

The samples thus obtained were washed thoroughly with distilled water by centrifugation at 3000 rpm and dried in a desiccator at 100 °C for three hours followed by heat treatment in a muffle furnace at 400 °C for one hour. The drying leaves only a precipitate of $Zn(OH)_2$, stabilised by surfactant. During the heat treatment, zinc hydroxide decomposes with the release of water (formula (4)) and pure ZnO powder is formed

$$Zn(OH)_2 \longrightarrow^{400\ ^{\circ}C} ZnO + H_2O \uparrow. \quad (4)$$

It should be noted that annealing improves crystallinity and removes residual organic impurities [19].

In the synthesis of ZnO by the modified microwave assisted method, 0.02 mol of zinc chloride ($ZnCl_2$, Sigma Aldrich) were dissolved in 200 mL of distilled water and stirred at 700 rpm without heating until complete homogeneity. Zinc chloride dissociated into ions in water according to formula (5)

$$ZnCl_2 \longrightarrow Zn^{2+} + 2Cl^{-}. \quad (5)$$

To the resulting solution, 30 ml of aqueous ammonia solution was added dropwise while still stirring the mixture. Immediately after addition, a white precipitate was formed. As addition proceeded, excess ammonia caused the precipitate to dissolve and an ammonia complex $[Zn(NH_3)_4]^{2+}$ was formed during reactions (6) and (7). Upon completion of the reactions, the solution became transparent.

$$Zn^{2+} + 4NH_3 + 4H_2O \longrightarrow 2Zn(OH)_2 \downarrow + 4NH_4^{+}, \quad (6)$$

$$Zn(OH)_2 + 4NH_3 \longrightarrow [Zn(NH_3)_4]^{2+} + 2OH^{-}. \quad (7)$$

The next step was microwave heating. The solutions were heated for 2.5 minutes at 350 W (sample #MW1), 5 minutes at 350 W (sample #MW2), 10 minutes at 350 W (sample #MW3), 15 minutes at 350 W (sample #MW4), 20 minutes at 350 W (sample #MW5), and 20 minutes at 70 W (sample #MW6) in an LG MS 1924x household microwave oven. Upon microwave heating of the tetraamminzinc solution $[Zn(NH_3)_4]^{2+}$ thermal decomposition of the complex occurs, accompanied by the release of ammonia and the formation of zinc oxide. The complex becomes unstable and decomposes into the ammonia gas phase, with zinc ions interacting with hydroxide ions to form an insoluble precipitate in the form of zinc oxide

$$[Zn(NH_3)_4]^{2+} + 2OH^{-} \longrightarrow^{\text{нагрев}} ZnO \downarrow + 4NH_3 \uparrow + H_2O. \quad (8)$$

After heating in microwave oven, the solution was cooled naturally at room temperature. After cooling, the solution was purified from impurities by centrifugation. In the last step, the solution was placed in a Petri dish and dried in a desiccator at 8°C.

Results and discussion

The morphological characteristics of the grown samples were examined using a Quanta 200i 3D electron scanning microscope (SEM) with a direct filament tungsten cathode (FEI, Hills Boro, Oregon, USA). This instrument provides images with a resolution of less than 2.5 nm and allows both qualitative and quantitative analyses of nanoscale structures. Figure 1 shows SEM images of the powders obtained by chemical bath deposition.

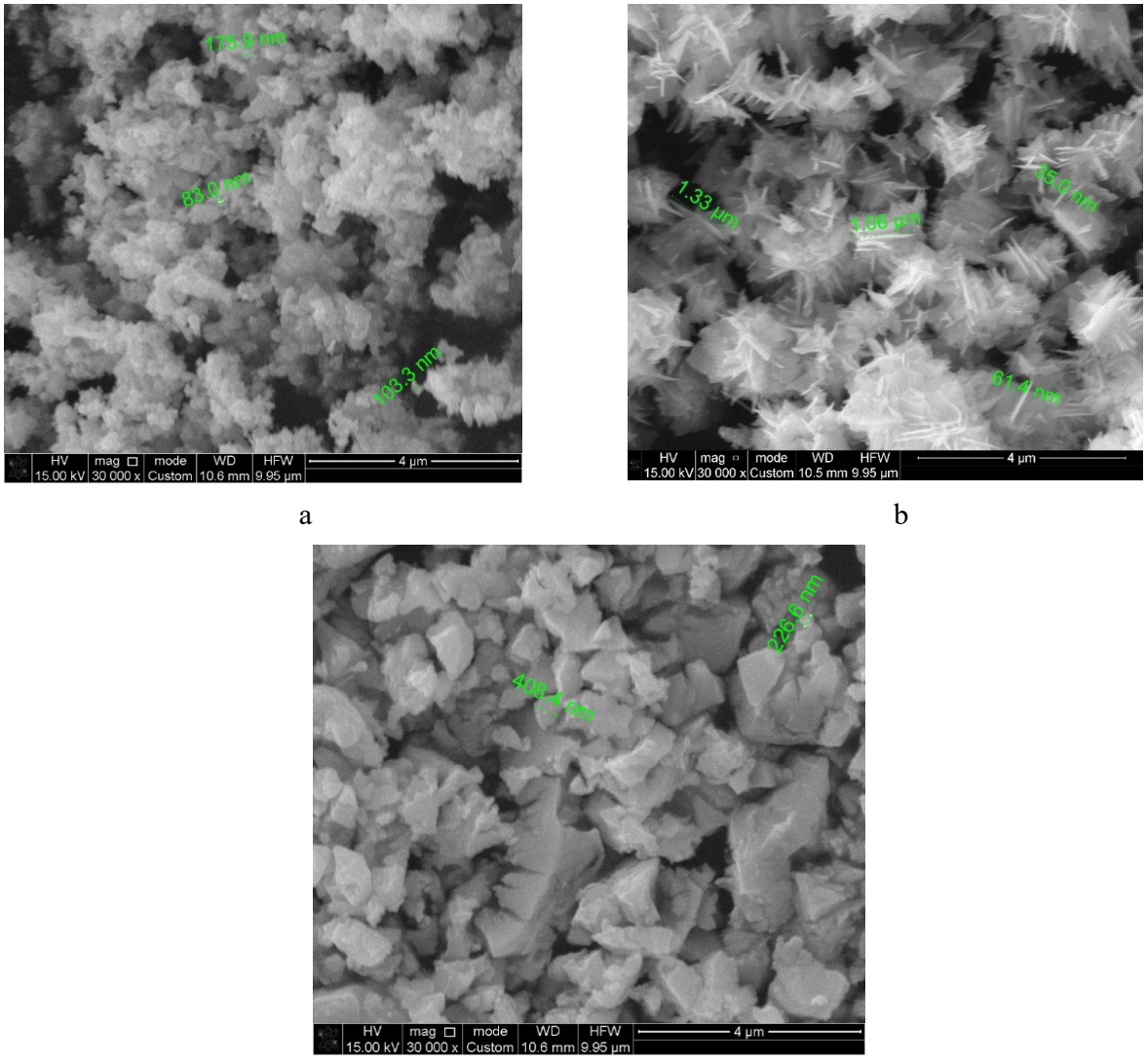

a b c

Figure 1 – SEM images of samples obtained by chemical deposition:
(a) sample #CD1, (b) sample #CD2, (c) sample #CD3

In Figure 1a, it is worth noting the polymorphic morphology including both quasi-spherical and polyhedral nanoparticles with characteristic sizes of 50–100 nm. This image shows a tendency towards agglomeration formation, with individual crystals exhibiting pronounced hexagonal symmetry, consistent with the wurtzite structure of ZnO. Of particular interest are the observed interparticle boundaries and in the form of cracks, which may be a consequence of capillary stresses arising during the sample drying process.

Figure 1b clearly shows highly anisotropic structures morphologically corresponding to nanowires or columnar crystals. The average diameter of these structures is 20–30 nm with lengths up to 500 nm. The directional growth mainly along the crystallographic axis [001] is a characteristic feature of the hexagonal modification of ZnO with high packing density. In Figure 1c it can be observed that the particles have irregular and angular shape with sharp edges, there are no pronounced crystals of hexagonal shape. Aggregates ranging in size from 200 nm to 1–2 μm can be seen. However, these aggregates are composed of smaller nanoparticles. This indicates secondary aggregation of small crystallites into larger structures. The particles are densely packed and a pronounced agglomeration characteristic of dry ZnO powders is observed. The surfaces of the particles appear rough and multifaceted, indicating the crystalline nature and good growth of individual facets. This may also be due to the formation of particles through nucleation and growth stages. The obtained morphological data are in agreement with literature data on characteristic shapes of ZnO nanocrystals, where the growth anisotropy is determined by differences in the surface energy of crystallographic planes of wurtzite structure [20].

Figure 2 shows SEM images of zinc oxide powders obtained by microwave assisted method at different synthesis parameters. It should be noted that the particles possess a flower-like morphology consisting of multiple elongated or lamellar crystallites with radial symmetry. This morphology is characteristic of self-organised nanostructures, often encountered in microwave synthesis, due to rapid heating and saturated growth of crystallites along certain crystallographic directions. The figures show that the size of a single "flower" varies between 2 and 5 μm. Individual elements within these aggregates - thin needle-like or lamellar crystals can vary from 100 to 500 nm in length and tens of nanometres in width. It should also be noted that the "flowers" are in close contact with each other, forming dense aggregations. Such agglomeration can be caused by the high surface energy of nanoparticles, rapid growth and deposition during microwave synthesis or the lack of stabilising agents.

It is noted that the sample #MW1 (Figure 2a) is characterised by the presence of predominantly spherical and weakly faceted nanoparticles of the order of 80-150 nm, forming loose agglomerates with high porosity. A short duration of heating leads to limited crystallite growth and partial preservation of amorphous sites, which in the long term can provide high specific surface area and activity of the material in adsorption and catalytic processes. Sample #MW2 (Figure 2b) contains particles with more pronounced hexagonal faceting characteristic of the wurtzite structure of ZnO. The crystallite size increases to 120–200 nm at a synthesis duration of 5 min, while particle agglomeration increases and porosity decreases.

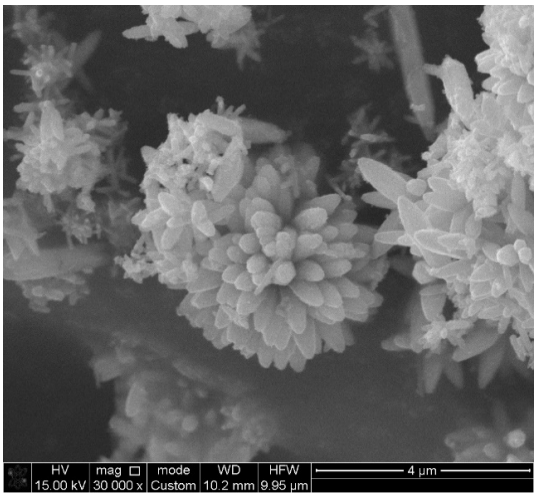

a

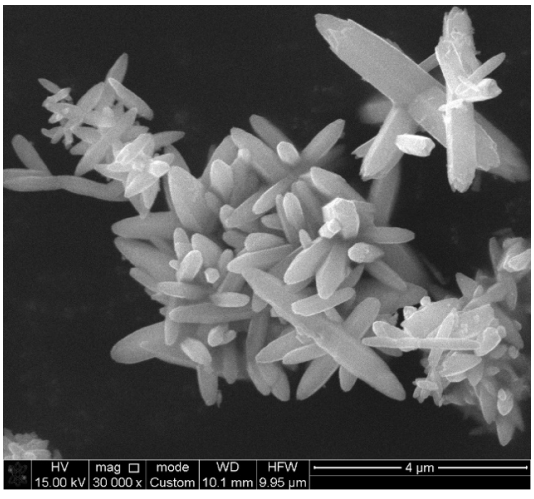

b

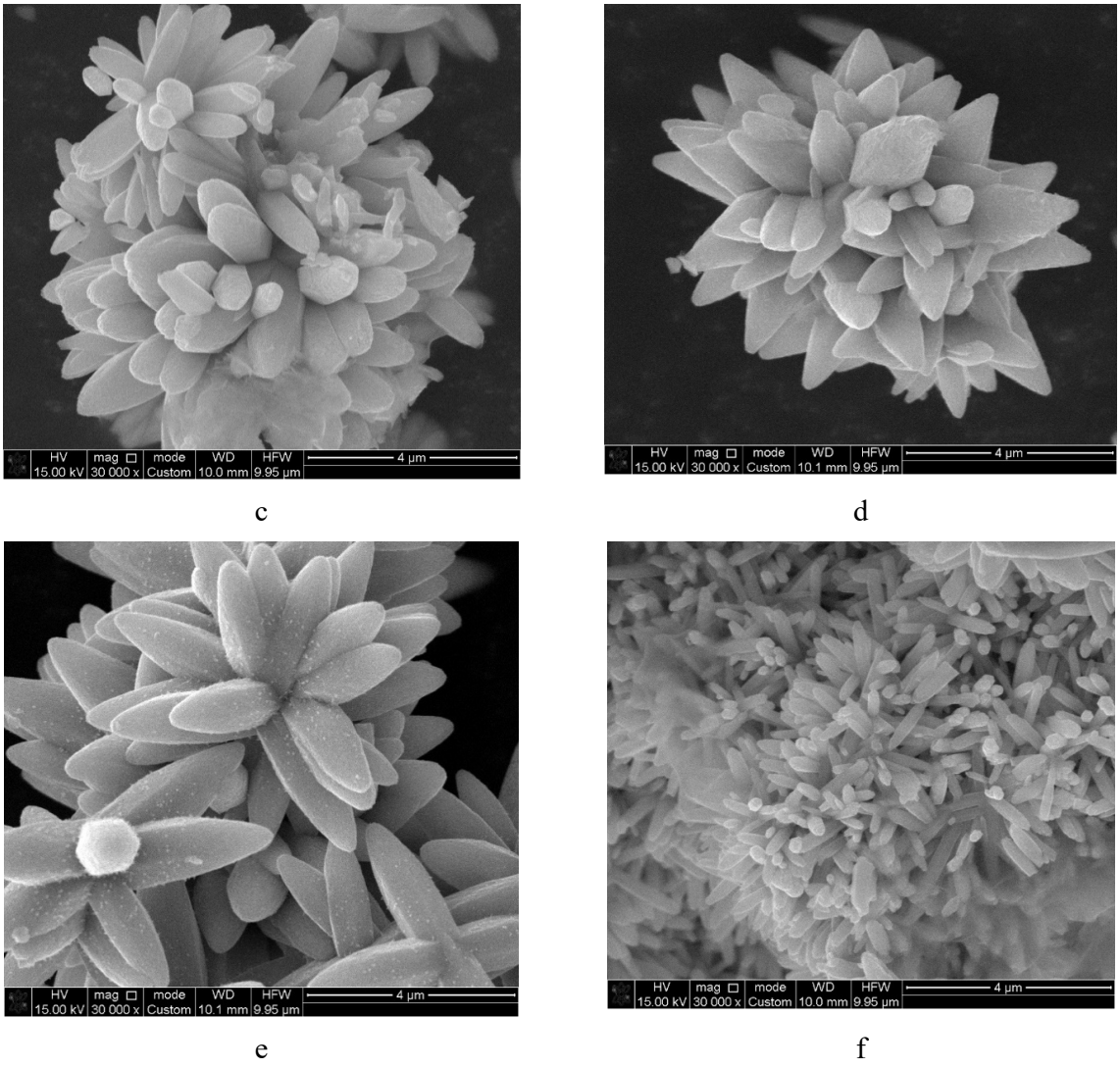

Figure 2 – SEM image of powder obtained by microwave assisted method at:
(a) sample#MW1, (b) sample #MW2, (c) sample #MW3, (d) sample #MW4,
(e) sample #MW5, (f) sample #MW6

The increase in the degree of crystallinity is due to more complete nucleation and growth processes at increasing microwave heating time. When the synthesis time is further increased up to 10 min, the formation of well-defined prismatic crystals of 200–300 nm length occurs (Figure 2c). In this case, the particles form dense aggregates, which indicates the activation of Ostwald ripening processes leading to crystallite enlargement and a decrease in specific surface area. In sample #MW4 (synthesis duration 15 min), well faceted prismatic and rod-like structures up to 500 nm in length were observed (Figure 2d). The high packing density and fusion of neighbouring particles in this sample indicate the predominance of directed crystal growth processes.

The morphology of sample #MW4 acquires features characteristic of evolved one-dimensional ZnO structures, which may be promising for optoelectronic and sensor applications. At the duration of microwave synthesis of zinc oxide of 20 min, the formation of elongated rod-shaped crystals of 0.5–1 μm length with smooth faces occurs (Figure 2e). Significant enlargement of particles and almost complete loss of porosity of this sample are due to the intensive growth of crystals under prolonged microwave exposure. These structures can provide high electron mobility, but their specific surface

area is significantly lower than that of samples with finer morphology. Reducing the power to 70 W allows crystals with lengths between 150 nm and 600 nm to be grown with a more reduced particle agglomeration (Figure 2f). The presence of interparticle voids indicates slower crystal growth and retention of an increased specific surface area, potentially enhancing the activity of the material in photocatalytic and sensing applications.

X-ray phase analysis of synthesised ZnO samples was performed on a Rigaku MiniFlex600 desktop X-ray diffractometer. Figure 3 shows the diffractograms of samples #CD1, #MW1 and #MW6. The analysis showed that all samples crystallise according to the hexagonal structure of wurtzite (card JCPDS 36-1451 — sample #CD1, card JCPDS 80-0075 — samples #MW1 and #MW6) with peaks characteristic of reflection planes (100), (002), (101), (102), (110), (103), (200), (112), (201),

corresponding to the hexagonal structure of wurtzite [21]. All three samples contain only ZnO phases, indicating high phase purity. It was observed that the synthesis method influences the texturisation, crystallite size and intensity of the diffraction peaks. In particular, the #CD1 sample obtained by chemical bath deposition shows the highest texturisation along the (101) direction. Such texturing is characteristic of isometric or aggregated particles growing without directional external influence. At the same time, samples #MW1 and #MW6 obtained by microwave assisted method are characterised by a more isotropic distribution of orientations, which is characteristic of fast microwave synthesis, in which crystallisation occurs under conditions of uniform heating and short growth time. It is worth noting that the peak width at half width (FWHM) of these samples is almost the same despite different synthesis parameters, indicating that microwave exposure provides efficient and uniform heating, and the final structure is determined by nucleation kinetics rather than stress. At high power (sample #MW1), rapid nucleation of centres occurs, resulting in the formation of small crystallites. At low power but for a long time (sample #MW6) an increase in limited diffusion, which also does not lead to a significant increase in size.

The photocatalytic activity of the obtained zinc oxide powders was investigated on a Cary Series UV-NIR spectrophotometer.

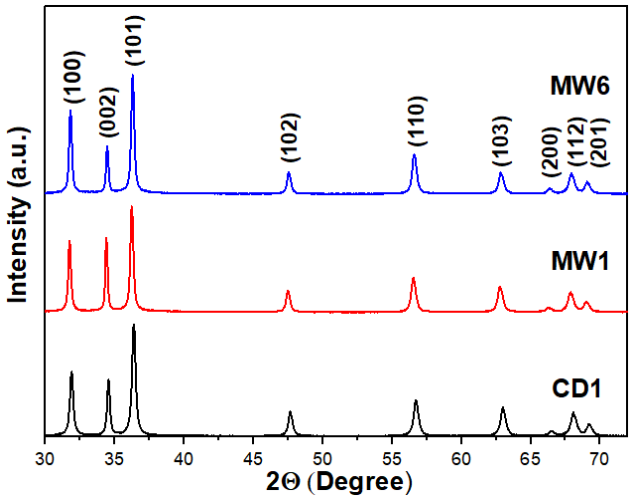

Figure 3 – X-ray diffraction patterns
of synthesised ZnO samples #CD1, #MW1 and #MW6

For the analysis, rhodamine-B was used as a dye. For this purpose, 9 mg of the investigated ZnO sample was added to 112.5 mL of aqueous dye solution. Firstly, the dye and powder were mixed on a magnetic stirrer at 700 rpm, then to increase dispersion they were treated for 30 minutes in an ultrasonic bath PSB-12808-05 without heating to increase dispersion. Exposure was carried out using a quartz lamp with a sampling interval of 30 minutes. Figure 4 shows the change in optical density spectra with increasing exposure time for samples #CD2 (Figure 4a) and #MW5 (Figure 4b).

In Figure 4, it can be observed that the maximum absorption intensity is observed at a wavelength of 545 nm, which corresponds to the absorption peak of rhodamine-B. The relative concentration of organic dye decreases with exposure time, which shows the high photocatalytic activity of the samples.

For a more accurate analysis, kinetic curves showing the dependence of the change in optical density of rhodamine-B solution on the exposure time are shown in Figure 5. The analysis of photocalytic degradation curves shows that sample #CD2 demonstrates the highest photocatalytic activity in the considered series at the average degradation rate $k_{av} \approx 0.5$ hr^{-1}, achieving a concentration reduction to ~30% of the initial concentration in 120 min.

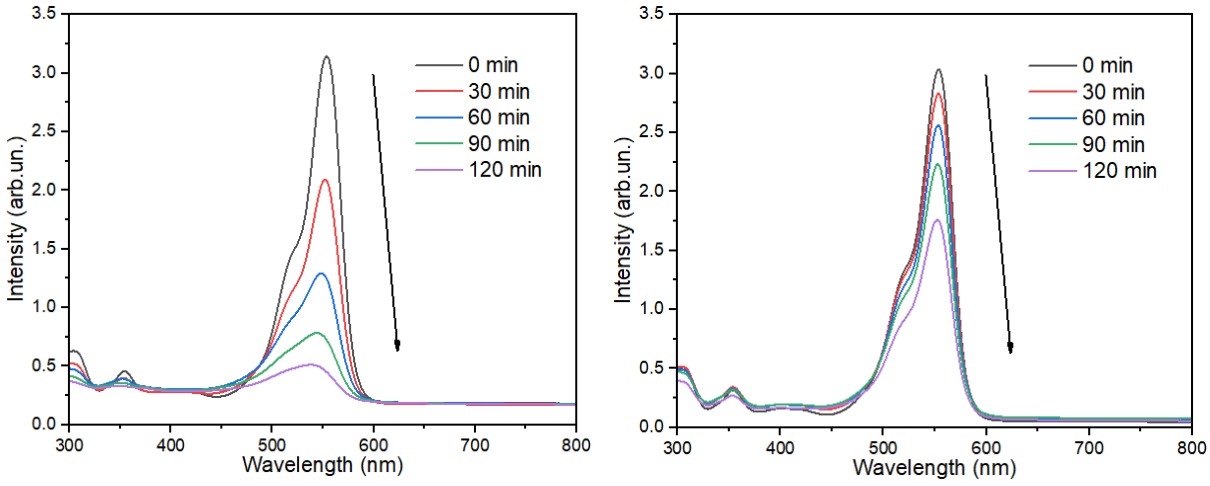

Figure 4 – Optical density spectra of ZnO samples: (a) #CD2, (b) #MW5

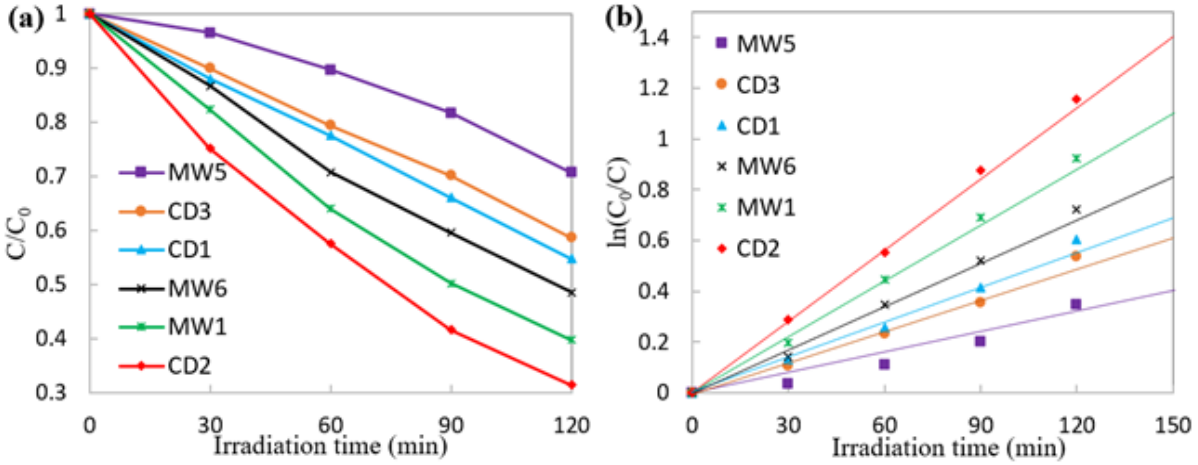

Figure 5 – Kinetic curves of dependence of absorption intensity on exposure time

This is probably due to the lamellar morphology of this sample and its high specific surface area providing efficient charge carrier transport. Slightly less high photocatalytic activity is possessed by sample #MW1 ($k_{av} \approx 0.4$ hr^{-1}) , which is due to the fine porous structure and high number of active centres on the surface involved in the photocatalytic decomposition of the dye. Despite somewhat inferior characteristics, the activity of powders obtained by the microwave assisted method can be significantly increased by optimising the synthesis conditions, in particular by introducing

surfactants to suppress agglomeration and reducing the heating power for more controlled crystal growth. Intermediate activity values are occupied by samples #MW6 and #CD1 ($k_{av} \approx 0.3$ hr^{-1}), which corresponds to their morphology - moderate particle sizes, presence of interparticle voids (#MW6) and polyhedral structure (#CD1). Sample #CD3 showed lower activity ($k_{av} \approx 0.2$ hr^{-1}), possibly due to dense agglomeration of particles and lower specific surface area. Sample #MW5 ($k_{av} \approx 0.1$hr^{-1}) showed the lowest photocatalytic efficiency, consistent with large rod-shaped crystals and almost no porosity. Thus, the key factors determining the photocatalytic activity of ZnO are particle size, degree of aggregation, specific surface area, and crystal growth anisotropy.

Conclusion

Thus, varying the molar concentration of $ZnAc_2$ using the chemical bath deposition method, other conditions of synthesis being equal, has a pronounced effect on the morphological characteristics of ZnO. An increase in concentration favours the formation of dense arrays of elongated nanostructures, whereas its decrease leads to the formation of loose and less ordered structures. These differences in morphology have the potential to significantly influence the optical and catalytic properties of the obtained materials. Moreover, comparative analysis of the obtained data showed that increasing the microwave heating time at constant power leads to the transition from loose nanostructures with high porosity to dense microstructures with low specific surface area. Decreasing the power at prolonged heating (#MW6) allows to slow down the crystallisation and aggregation processes, preserving a more finely dispersed and surface-developed structure. These results confirm the possibility of targeted regulation of morphology and, consequently, functional properties of ZnO by optimising microwave synthesis parameters. The sample of zinc oxide #CD2 synthesised by chemical bath deposition showed higher characteristics both in terms of morphological parameters, such as reduced average particle size and lower degree of agglomeration, and in terms of photocatalytic activity. The results obtained allow for a greater degree of control of morphology and crystallite size in the synthesis of ZnO to optimise its photocatalytic properties. Nanoplatelet and fine morphology (#CD2, #MW1) provides the highest activity due to the developed surface and directional transport of charge carriers. Large single-crystal structures with low porosity (#MW5) show the minimum efficiency. Reduced microwave heating power (#MW6) preserves the fine structure and moderate activity, making this regime promising for photocatalytic applications. The synthesised photocatalytically active samples are promising for water purification from organic contaminants in food, textile industries, as well as in sensor applications.

Funding information: The study was carried out with the financial support of the Ministry of Science and Higher Education of the Republic of Kazakhstan (grants No AP23488569 and AP26103537).

REFERENCES

1 Zhao, Z., Agulto, V.C., Iwamoto, T., Kato, K., Yamanoi, K., Shimizu, T., Sarukura, N., Fujii, T., Fukuda, T., Yoshimura, M., Nakajima, M. Investigation of the optical and electrical properties of zinc oxide by terahertz time domain ellipsometry. Optical Materials: X, 24, 100352 (2024). https://doi.org/10.1016/j.omx.2024.100352.

2 Pavan Kumar, M.A., Suresh, D., Sneharani, A.H. Centella asiatica mediated facile green synthesis of nano zinc oxide and its photo-catalytic and biological properties. Inorganic Chemistry Communications, 133, 108865 (2021). https://doi.org/10.1016/j.inoche.2021.108865.

3 Abdullin, A.Kh., Cicero, G., Gritsenko, L.V., Kumekov, S.E., Markhabaeva, A.A. Effect of annealing and hydrogen plasma treatment on the luminescence and persistent photoconductivity of polycrystalline ZnO films. Journal of Applied Physics, 121, 245303-1–245303-6 (2017). https://doi.org/10.1063/1.4989826.

4 Haygood, K.J.F., Dinny Harnany, Jamasri, Santos, G.N.C., Muflikhun, M.A., Promising CO2 gas sensor application of zinc oxide nanomaterials fabricated via HVPG technique. Heliyon, 10 (17), e36692 (2024). https://doi.org/10.1016/j.heliyon.2024.e36692.

5 Olavo Cardozo, Ricardo Maia-Junior, Sajid Farooq, Braulio Tostes, Andreas Stingl, Patricia Farias, Severino Alves Junior, Zinc oxide nanostructures for third generation solar cells: A comprehensive review, Solar Energy, 299, 113710 (2025). https://doi.org/10.1016/j.solener.2025.113710.

6 Kedruk, Y.Y., Contestabile, A., Zeng, J., Fontana, M., Laurenti, M., Gritsenko, L.V., Cicero, G., Pirri, C.F., Abdullin, K.A. Morphology Effects on Electro- and Photo-Catalytic Properties of Zinc Oxide Nanostructures. Nanomaterials, 13, 2527 (2023). https://doi.org/10.3390/nano13182527.

7 Rana, A., Kumar, P., Thakur, N., Kumar, S., Kumar, K., Thakur, N. Investigation of photocatalytic, antibacterial and antioxidant properties of environmentally green synthesized zinc oxide and yttrium doped zinc oxide nanoparticles. Nano-Structures & Nano-Objects, 38, 101188 (2024). https://doi.org/10.1016/j.nanoso.2024.101188.

8 Ulker, G., Penlik, Y., Gorduk, S. Synthesis, characterization and investigation of photocatalytic activity of ZnO Nanoparticles from Tilia Tomentosa (silverly linden) plant by green synthesis method. Journal of Molecular Structure, 1344, 142929 (2025). https://doi.org/10.1016/j.molstruc.2025.142929.

9 Arepalli, V.K., Yang, E., Patil, A.A., Wi, J.-S., Park, J.S., Lee, J.-M., Lee, S., Chung, Ch.-H. ZnO nanowire broadband ultra-wide-angle optical diffusers grown by aqueous chemical bath deposition. Journal of Alloys and Compounds, 1008, 176660 (2024). https://doi.org/10.1016/j.jallcom.2024.176660.

10 Gilani, S.E.H., Younas, M., Nazar, R., Rasheed, M.H., Mehmood, U. Microwave-assisted synthesis of ZnO nanostructured photoanodes for advanced dye-sensitized solar cells. Materials Letters, 400, 139146 (2025). https://doi.org/10.1016/j.matlet.2025.139146.

11 Rustembekkyzy, K., Sabyr, M., Kanafin, Y.N., Khamkhash, L., Atabaev, T.Sh. Microwave-assisted synthesis of ZnO structures for effective degradation of methylene blue dye under solar light illumination. RSC Advances, 14 (23), 16293–16299 (2024). https://doi.org/10.1039/d4ra02451f.

12 Ahmed, M., Coetsee, L., Goosen, W.E., Urgessa, Z.N., Botha, J.R., Venter, A. Characterization of Bi-doped ZnO nanorods prepared by chemical bath deposition method. Physica B: Condensed Matter, 666, 415105 (2023). https://doi.org/10.1016/j.physb.2023.415105.

13 Zhu, J., Feng, Y., Dai, B., Qi, Y. Morphology and orientation controlling of ZnO nanofibers via chemical bath deposition. Materials Chemistry and Physics, 305, 128028 (2023). https://doi.org/10.1016/j.matchemphys.2023.128028.

14 Sandhu, G.S., Nine, M.J., Purasinhala, K., Dadkhah, M., Hassan, K., Losic, D. Morphology and charge effect of ZnO nanostructures on the performance of anticorrosion coatings. Surfaces and Interfaces, 69, 106750 (2025). https://doi.org/10.1016/j.surfin.2025.106750.

15 Alp, E., Olivieri, F., Aulitto, M., Castaldo, R., Contursi, P., Cocca, M., Gentile, G. The effect of ZnO nanoparticles morphology on the barrier and antibacterial properties of hybrid ZnO/graphene oxide/montmorillonite coatings for flexible packaging. Surfaces and Interfaces, 55, 105307 (2024). https://doi.org/10.1016/j.surfin.2024.105307.

16 Kowalik, P., Konkol, M., Antoniak-Jurak, K., Próchniak, W., Wiercioch, P., Rawski M., Borowiecki T. Structure and morphology transformation of ZnO by carbonation and thermal treatment. Materials Research Bulletin, 65, 149–156 (2015). https://doi.org/10.1016/j.materresbull.2015.01.032.

17 Tolubayeva, D.B., Gritsenko, L.V., Kedruk, Y.Y., Aitzhanov, M.B., Nemkayeva, R.R., Abdullin, K.A. Effect of hydrogen plasma treatment on the sensitivity of ZnO based electrochemical non-enzymatic biosensor. Biosensors, 13, 793 (2023). https://doi.org/10.3390/bios13080793.

18 Uribe-López, M.C., Hidalgo-López, M.C., López-González, R., Frías-Márquez D.M., Núñez-Nogueira G., Hernández-Castillo D., Alvarez-Lemus M.A. Photocatalytic activity of ZnO nanoparticles and the role of the synthesis method on their physical and chemical properties. Journal of Photochemistry and Photobiology A: Chemistry, 404, 112866 (2021). https://doi.org/10.1016/j.jphotochem.2020.112866.

19 Hussein S.N.C.M., Fuad F.S.M., Ismail M. Synthesis of zinc oxide nanoparticles for oil upgrading and wax deposition control: effect of calcination temperature. Indonesian Journal of Chemistry, 20 (4). 746–754 (2020). https://doi.org/10.22146/ijc.43317.

20 Dobrozhan, O., Shelest, I., Stepanenko, A., Kurbatov, D., Yermakov, M., Čerškus, A., Plotnikov, S., Opanasyuk, A., Structure, substructure and chemical composition of ZnO nanocrystals and films deposited onto flexible substrates. Materials Science in Semiconductor Processing, 108, 2020, 104879, https://doi.org/10.1016/j.mssp.2019.104879.

[1]Қадау А.Т.,
магистр, ORCID ID: 0009-0008-9714-0304,
e-mail: aidoskadau@gmail.com
[1,2]Калкозова Ж.К.,
к.ф-м.н., ассоциированный профессор, ORCID ID: 0000-0002-4826-1678,
e-mail: zhanar.kalkozova@kaznu.edu.kz
[1,3]*Гриценко Л.В.,
PhD, ассоциированный профессор, ORCID ID: 0000-0003-0726-1118,
*e-mail: l.gritsenko@satbayev.university
[1,2]Мархабаева А.А.,
PhD, ORCID ID: 0000-0002-0657-422X,
e-mail: aiko.marx87@gmail.com
[1,2]Абдуллин Х.А.,
д.ф-м.н., профессор, ORCID ID: 0000-0002-2729-2272,
e-mail: kh.abdullin@physics.kz

[1]Институт прикладных наук и информационных технологий, г. Алматы, Казахстан
[2]Национальная нанотехнологическая лаборатория открытого типа (ННЛОТ),
Казахский национальный университет имени аль-Фараби, г. Алматы, Казахстан
[3]Satbayev University, г. Алматы, Казахстан

ВЛИЯНИЕ ПАРАМЕТРОВ НИЗКОЗАТРАТНЫХ МЕТОДОВ СИНТЕЗА НА МОРФОЛОГИЮ ОКСИДА ЦИНКА

Аннотация

Исследована морфология порошков оксида цинка (ZnO), синтезированных модифицированным микроволновым методом при различных параметрах нагрева и методом химического осаждения. Анализ изображений позволил установить закономерности формирования структуры в зависимости от параметров синтеза. Показано, что увеличение времени микроволнового нагрева при постоянной мощности приводит к последовательному переходу от рыхлых наночастиц к плотным, хорошо ограненным микроструктурам. Кроме того, снижение мощности нагрева замедляет процессы кристаллизации и агломерации, сохраняя более мелкодисперсную и пористую структуру. Сканирующая электронная микроскопия выявила также существенные различия в морфологии образцов, выращенных методом химического осаждения, обусловленные изменением исходной молярной концентрации ацетата цинка при фиксированных концентрациях остальных компонентов раствора роста. Таким образом, представлены низкозатратные, экологичные, контролируемые методы синтеза образцов ZnO, позволяющие направленно управлять морфологией частиц за счет изменения концентрации прекурсоров, оптимизации времени и мощности микроволнового синтеза. Показана возможность применения выращенных структур для фотокаталитического разложения органического красителя родамина-В. Установлена взаимосвязь между скоростью фотокаталитического разложения и морфологией частиц оксида цинка. Наибольшая скорость фотокаталитической деградации родамина-В ≈ 0.5 hr^{-1} в рассмотренной серии зафиксирована у образца, полученного методом химического осаждения, наименьшая ≈0.1 hr^{-1} – у образца, синтезированного микроволновым методом.

Ключевые слова: оксид цинка, морфология, микроволновый метод, метод химического осаждения, фотокатализ.

Article submission date: 14.08.2025